

Learning to Reorient Objects with Stable Placements Afforded by Extrinsic Supports

Peng Xu, Hu Cheng, Jiankun Wang*, *Senior Member, IEEE*, and Max Q.-H. Meng*, *Fellow, IEEE*

Abstract—Reorienting objects using extrinsic supporting items on the working platform is a meaningful nonetheless challenging manipulation task, considering the elaborate geometry of objects and the robot’s motion planning. In this work, the robot learns to reorient objects through sequential pick-and-place operations according to sensing results from the RGBD camera. We propose generative models to predict objects’ stable placements afforded by supporting items from observed point clouds. Then, we build manipulation graphs which enclose shared grasp configurations to connect objects’ stable placements for pose transformation. We show in experiments that our method is effective and efficient. Simulation experiments demonstrate that the models can generalize to previously unseen pairs of objects started with random poses on the table. The calculated manipulation graphs are conducive to provide collision-free motions to reorient objects. We employ a robot in the real-world experiments to perform sequential pick-and-place operations, indicating our method is capable of transferring objects’ placement poses in real scenes.

Note to Practitioners—Reorienting objects is a common manipulation task in daily and factory scenarios. Extrinsic objects are used as supporting items to provide placements for the query objects and then provide grasp configuration space for the robot. Previously, mesh models of objects are required for calculating stable placements and building manipulation graphs. In this work, a data-driven method is proposed to predict various placements based on the perception results of point clouds from the RGBD camera, capable of generalizing to novel objects in new scenes. We also build manipulation graphs based on point clouds, which relax motion planning of the robot and contain collision-free pick-and-place operations for the robot to reorient objects to stable placements afforded by supports. In the future, we will improve the performance of our method by improving the performance of the distance metric between pose sets.

Index Terms—Object reorientation, Deep learning, Manipulation graph.

I. INTRODUCTION

REORIENTING objects using external supports [1] is an important skill for robots in not only domestic scenes

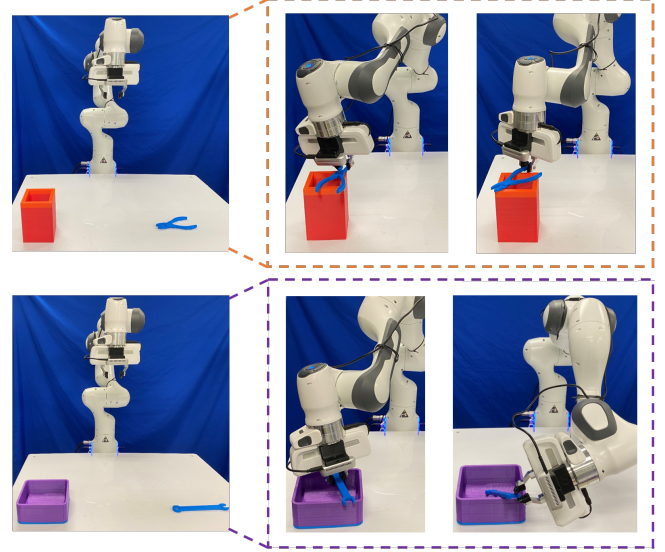


Fig. 1. Examples of reorientation. The robot reorients objects to placement poses afforded by supports, based on the perception of scenes with the camera mounted on the robot’s hand. After reorientation, the robot grasps the objects’ surface area unreachable in the initial scene owing to the collision between the gripper and the table, or the area covered by the working platform in the initial scene. This way, the robot can use tools dexterously.

but also industrial scenes when robots are unable to manipulate objects to goal poses for grasping directly. Due to the kinematic constraints of the robot arm, the obstruction caused by the working platform, and the elaborate geometry of the object, the robot needs to reorient the object with the supporting items to placement poses for grasping the uncovered area. The supporting items are crucial to providing stable intermediate placements of the object for sufficient motion space in sequential pick-and-place manipulation steps adopted by the robot. Therefore, the robot grasps the object’s functional area covered or affected by the table previously.

Different from the in-hand manipulation methods [2], [3] that employ dexterous hands to adjust objects’ poses, the extrinsic manipulation methods [4], [5] utilize the supporting items that can provide stable placement poses for easy robotic grasp configurations. As depicted in Fig. 1, the robot reorients rigid objects using stable intermediate placements afforded by supports, that is, the holder and the container in the figures. In the top row, after reorientation, the robot can grasp the plier deeply relative to the tip at one placement and grasp the handle exposed at another placement. Similarly, in the bottom row, the robot can grasp the wrench deeply at the first placement and

*Corresponding authors: Jiankun Wang, Max Q.-H. Meng.

Peng Xu and Hu Cheng are with the Department of Electronic Engineering, The Chinese University of Hong Kong, Hong Kong {peterxu, hcheng}@link.cuhk.edu.hk

Jiankun Wang is with the Department of Electronic and Electrical Engineering of the Southern University of Science and Technology in Shenzhen, China wangjk@sustech.edu.cn

Max Q.-H. Meng is with the Department of Electronic and Electrical Engineering of the Southern University of Science and Technology in Shenzhen, China, on leave from the Department of Electronic Engineering, The Chinese University of Hong Kong, Hong Kong, and also with the Shenzhen Research Institute of the Chinese University of Hong Kong in Shenzhen, China max.meng@ieee.org

grasp the revealed end of the wrench at the second placement. As these supports provide enough grasping space for the robot arm, the robot is able to contact the areas on objects that are unavailable on the flat table. Overall, the key components for solving reorientation manipulation are proposing the query objects' stable placements with supporting items and planning sequential pick-and-place steps for placements transformation.

Wan *et al.* [1] calculate the stable placements of wooden blocks on the flat table based on their mesh models and build two-layer grasp graphs to connect these stable placements with calculated grasp configurations of the specific gripper. However, the method is limited to objects with simple and known geometry. Ma *et al.* [5] utilize the Bullet simulator for the simulation process to obtain stable placements of objects with complex supports. Although they build grasp graphs in parallel with the simulation process, the method requires detailed mesh models of both objects and supports loaded into the simulation. Several works [6]–[8] push or pivot objects while keeping objects in the robot's hands. Nevertheless, these methods are unable to operate or build dexterous manipulation graphs without physical information of objects, e.g., the friction, masses, and mesh models.

The deep learning methods have the ability to generalize learned models to unseen objects based on the perception results from sensors like RGBD cameras and achieve promising results. In [9], with the perceived point clouds, the stable hanging pose of the object is predicted by regressing key contact points on both the query object and the support. However, the regression result is usually one stable pose for the hanging task, which is limited for building manipulation graphs of reorienting objects. Paxton *et al.* [10] use point clouds of stable poses and unstable poses to train the discriminator for the scene classification. Our work trains generative models to propose multiple stable placement poses of the query object by learning from stable poses and unstable poses. We also train discriminators using stable point clouds and unstable point clouds to avoid penetration cases.

Our contributions are as follows. (1) We proposed generative models which directly compare placement pose sets, taking one perceived point cloud of the whole scene as input. (2) To our best knowledge, we are the first to build manipulation graphs based on point clouds, which enclose sequential pick-and-place operations for reorienting objects. (3) We generated a large-scale dataset including point clouds of stable placements and unstable poses, which embraces almost all the contact cases between objects.

II. RELATED WORK

Reorienting objects can be accomplished in two main different ways. One way is to use dexterous hands and the control policy to change the poses of objects in hand without extrinsic supports. There are several works on in-hand manipulation [2], [3], [11], which incorporate dexterous end-effectors and the manipulation policy obtained through imitation learning [2], reinforcement learning [3], or optimization methods [11] to adjust the position of objects in hand. The other way is to use placement poses provided by extrinsic supporting items,

simple as a desktop [1] or complex as a container [5] and another gripper [6], [7]. The robot plays the part of transforming objects' poses. Usually, the robot's motion planning contains sequential operations to adjust objects' poses. We also discuss relevant works on building manipulation graphs of sequential manipulation operations.

There are several works [6], [7], [12]–[14], which proposed to reorient objects with two robot arms. These methods can change the poses of objects in the air with the help of the supporting gripper. When performing object reorientation, [12] handovers objects between two grippers without transferring the poses of the object relative to the grippers. While [6], [7], [13] push the object grasped in one end-effector using another end-effector.

Wan *et al.* [1], [15] propose to adjust the poses of objects on the flat table surface using a single robot arm, given mesh models of objects and the gripper. They calculate the convex hulls of the query objects and compute objects' stable placements on a horizontal table as the support. Hou *et al.* [8], [16] adopt pivoting, which is a manipulation primitive that relies on the gripper model and contact constraints, for reorienting tasks. The objects are contacted with the gripper and the working platform in the pivoting process. Mesh models are needed for mechanical analysis. Some works take complex supports into consideration for obtaining stable placements of objects. Cao *et al.* [4] use a vertical pin to support the query object and compute stable placements that are different from poses supported by the horizontal surface. At the same time, they focus on the relatively simple support. It is still challenging to find objects' stable placement poses on other complex supports. Ma *et al.* [5] use the Bullet dynamic simulator to directly get the query object's stable placements on the complex support by free drop trials. However, this approach is time-consuming and needs detailed physical information for accurate simulation results, such as masses of models and their friction.

There are also some works that utilize data-driven methods for generalization to unseen objects to obtain the object's stable placements on the complex supports based on the sensor perception. Given the point clouds of objects, Jiang *et al.* [17], [18] manually design features representation and use the Support Vector Machine to find objects' placements on several supports. The work [19] proposes a constructive learning method considering stable and unstable poses to obtain the placement pose of various objects. Fox *et al.* [10] solve the rearrangement task to place objects under semantic instructions. They also use the stable and unstable point clouds poses of the query objects to train the discriminator for placements classification. We follow a similar idea and train classifiers to discriminate placements with supports and unstable poses. The work [10] determines the placement pose of the query object satisfying a particular relationship by the optimization approach. In our work, we leverage a multi-stage prediction method to generate as well as refine diverse stable placements of objects. In [9], [20], the object's placements are found by regressing the contact points on the object and the support. The position relationship of the object-support pair is considered, while the supporting effect of the table is ignored.

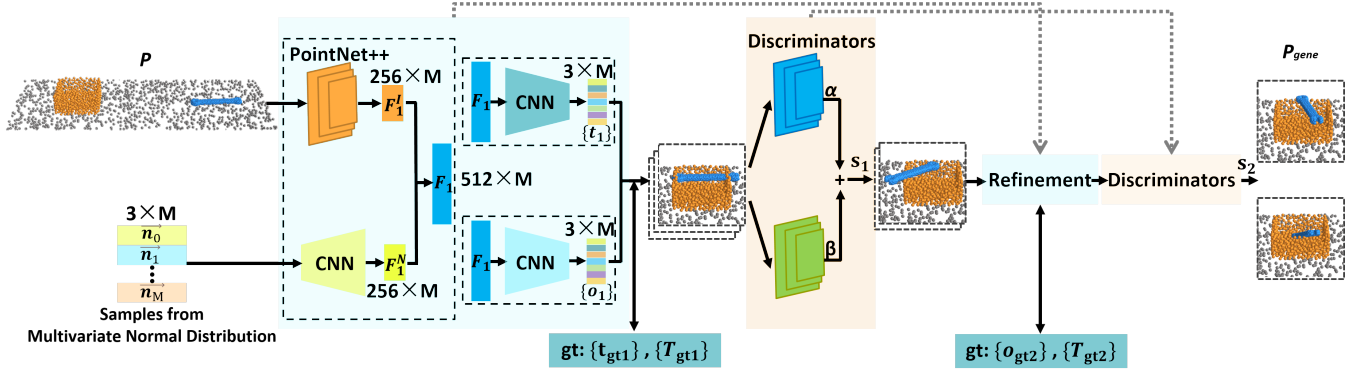


Fig. 2. The overview of the pipeline for stable placements prediction. The input includes the segmented point clouds \mathcal{P} of the scene and random noise samples $\{\vec{n}\}$. We leverage a two-stage prediction method to generate and refine diverse stable placements. Specific loss functions are designed for each stage. In the first stage, the wrench's (blue) poses close to the support (orange) are proposed. We then evaluate the stability and diversity of the generated point clouds. After the refinement stage, point clouds \mathcal{P}_{gene} of the transformed object with new poses and the preserved supporting environment are output.

When considering the kinematics of the robot with a fixed base in the scene, a single placement pose is not sufficient for reorienting tasks.

Quite a few works choose to adjust the object's poses through sequential operations. In addition to inferring the stable poses of the object, the key to the implementation is motion planning for pose transformation. In various works, manipulation graphs are built with intermediate states of the objects to be manipulated and calculated motion configurations of the robot for transferring the objects' states in a collision-free way. After calculating stable placements of the object on the table, Wan *et al.* [1] build a two-layer regrasping graph, in which the first layer shows connectivity between two stable placements and the second layer shows shared grasp configurations. Ma *et al.* [5] build the regrasping graph in parallel with the simulation process of obtaining the object's stable poses. The simulation process costs a longer period to obtain more stable placements added to the manipulation graph. Haustein *et al.* [6], [7] move the object to a new pose by pushing the object in hand as per the dexterous manipulation graph with optimized grasp configurations. In [8], [16], motion primitives like rolling, pivoting, and pick-and-place are used to construct manipulation graphs. However, these approaches require detailed mesh models of objects. In our work, motion primitives are computed based on the input point clouds to generate manipulation graphs. We also take the support as the anchoring object, and the world frame is established at the support bottom to simplify the computation.

III. APPROACH

Given the point cloud generated using multi-view images of the current scene, including the object, the supporting item, and the table surface, our goal is to propose the object's stable placements with supports and compute the robot's grasp configurations reorienting the object through several pick-and-place steps.

Using methods introduced in [21], the input point cloud is the segmented point cloud \mathcal{P} with a label channel added to each point for identifying the query object p_q and the supporting environment p_s . Inspired by the technique in

Generative Adversarial Networks [22], we also take samples $N = \{\vec{n}\}$ from random distribution as input to avoid the results converging to a single pose and let our models fit the distribution over stable placement poses. We adopt a two-stage process to predict transformation poses $\{\mathbf{T}\}$ for the query object p_q , which are comprised of 3D translation variation $\{t = (\Delta x, \Delta y, \Delta z)\}$ and 3D Euler angle variation $\{o = (\Delta \alpha, \Delta \beta, \Delta \gamma)\}$ with respect to the world frame. We introduce our models in detail in Sec. III-A and describe the details of the generated dataset in Sec. III-C. Then, the resulting placements \mathcal{P}_{gene} constructed by the transferred point clouds p'_q and constant point clouds p_s are nodes considered for building the manipulation graph. On account of the generated placements \mathcal{P}_{gene} and the rigid transformation $\{\mathbf{T}\}$, we compute grasp configurations that are shared by two placements in the manipulation graph. The relative pose between the parallel-jaw gripper \mathcal{M} and the query object is invariable in each pick-and-place step. We explain the detailed construction process of the manipulation graph in Sec. III-B.

A. Placement Prediction Models

An overview of our pipeline is depicted in Fig. 2. We train deep neural networks to predict the transformation poses of the query object from initial poses to stable placement poses. To this end, generative models are trained to learn the distribution of objects' stable placement poses afforded by supports, and pose classifiers are trained for selecting placements of convincing accuracy scores.

We take as given the segmented point clouds $\mathcal{P} \in \mathbb{R}^{2048 \times 4}$ of the scene with 2048 points, where the supporting item is kept stationary, and the query object next to it is placed on the table with a random initial pose. In the first stage, a PointNet++ [23] encoder $e(\mathcal{P})$ is used to extract a 256-dimensional feature vector f_1^I of the initial point clouds. This feature vector is duplicated as F_1^I to match with input of the random noise. As mentioned before, we also sample M random variables $N_1 \in \mathbb{R}^{3 \times M}$ from a multivariate normal distribution $\mathcal{N}(\vec{\mu}, \sigma^2 \mathbf{I})$ parameterized by a zero mean vector $\vec{\mu}$ and a covariance matrix $\sigma^2 \mathbf{I}$. We then use an upsampling module which consists of two convolutional layers as fully

connected layers to map these samples from the input size to a feature representation F_1^N of dimension $256 \times M$. Next, we concatenate F_1^N with the repeated latent representation F_1^I of dimension $256 \times M$ to obtain a feature map F_1 of dimension $512 \times M$ as inputs, and then use two separate downsampling modules which consist of four convolutional layers to output 3D translation $t_1 \in \mathbb{R}^{3 \times M}$ and 3D orientation $o_1 \in \mathbb{R}^{3 \times M}$, respectively.

The above network is trained with ground truth 6D placement poses, as described in Sec. III-C, which are the point set of the coordinates of poses. We design loss functions based on the Chamfer distance [24], which compares two point sets S_1 and S_2 as:

$$d_{CD}(S_1, S_2) = \sum_{x \in S_1} \min_{y \in S_2} \|x - y\|_2^2 + \sum_{y \in S_2} \min_{x \in S_1} \|x - y\|_2^2. \quad (1)$$

In the first stage, we let the network learn to move the query object close to the anchoring support. The scales and impact of the translation coordinates, compared with the orientation coordinates, are different in determining the placements of the query object. So we use the Chamfer distance of 3D translation poses $\{t_{gt1}\}$ and the Chamfer distance of 6D placement poses $\{\mathbf{T}_{gt1}\}$ to train the first generative network. We denote the distance of the translation poses as $d_{CD}(\{t_1\}, \{t_{gt1}\})$ in \mathbb{R}^3 , and the distance of placement poses as $d_{CD}(\{\mathbf{T}_1\}, \{\mathbf{T}_{gt1}\})$ in \mathbb{R}^6 , respectively. Thus, the loss function of the first stage is

$$\mathcal{L}_1 = d_{CD}(\{t_1\}, \{t_{gt1}\}) + d_{CD}(\{\mathbf{T}_1\}, \{\mathbf{T}_{gt1}\}). \quad (2)$$

Based on the prediction poses $\{\mathbf{T}_1\}$, we transfer the query object to new poses to obtain the transferred point clouds. We then train two discriminators to score the transformed point clouds separately. One is to learn the boundary between stable placements and near stable but unstable poses. The other is to learn the boundary between the stable placements and penetration poses. Then we obtain the weighted score s_1 , where α and β are weights for each score. Each discriminator is a PointNet++ network followed by Multilayer Perceptron, which takes as input the transformed point clouds and outputs the corresponding probabilities of two classes. We formulate the scoring process as a binary classification of stable and unstable placements. The supervised data of point clouds with stable labels and unstable labels are introduced in Sec. III-C. We adopt the loss

$$\mathcal{L}_{class} = -\mathbf{x}[l] + \log(\exp(\mathbf{x}[0]) + \exp(\mathbf{x}[1])) \quad (3)$$

for training, where l is the index of the ground truth label, and \mathbf{x} is the prediction vector for the two classes.

We not only set a threshold for s_1 , but also define a distance d based on Earth Mover's distance [25] to choose placements with variance. The distance d takes the form

$$d = \frac{d_{EMD}(p'_q, p''_q)}{\text{len}(p_q)L(p_s)}, \quad (4)$$

where p'_q and p''_q are transformed point clouds of the query object, $\text{len}(p_q)$ is the number of the query object's points, and $L(p_s)$ is the length of furthest two points on the support. We use d to represent the difference between any two placements

of a specific object-support pair. In the first stage, we set a threshold δ_1 for selecting dissimilar predictions.

In order to obtain stable placements for building manipulation graphs, we utilize a refinement stage to adjust the placement poses generated from the former stage. We also find that the second stage can generate diverse stable placements based on a prediction from the first stage. Thus, the number of placements increases after the second stage. The network architecture of refinement is similar to the previous stage. Distinctly, we use the Chamfer distance of 3D orientation poses $\{o_{gt2}\}$ and the Chamfer distance of 6D placement poses $\{\mathbf{T}_{gt2}\}$ between unstable poses and stable poses for training. We denote the distance of the orientation poses as $d_{CD}(\{o_2\}, \{o_{gt2}\})$ in \mathbb{R}^3 , and the distance of placement poses as $d_{CD}(\{\mathbf{T}_2\}, \{\mathbf{T}_{gt2}\})$ in \mathbb{R}^6 , respectively. The loss function of the second stage is

$$\mathcal{L}_2 = d_{CD}(\{o_2\}, \{o_{gt2}\}) + d_{CD}(\{\mathbf{T}_2\}, \{\mathbf{T}_{gt2}\}). \quad (5)$$

Similarly, the refined point clouds are also scored by the two discriminators. We set thresholds for the score s_2 and the distance δ_2 to select \mathcal{P}_{gene} . The generative models and discriminator models are trained separately.

B. Manipulation Graph Establishment

Algorithm 1: Manipulation graph building

Input: the point cloud of the query object p_q , the point clouds of the supporting environment p_s , the model of the default gripper \mathcal{M} .

Output: the manipulation graph \mathcal{G} revealing sequential pick-and-place operations

```

1  $\mathcal{G}.\text{init}(p_q, p_s)$ 
2  $\mathcal{E}_{inter} \leftarrow \emptyset, \mathcal{E}_{intra} \leftarrow \emptyset, \mathcal{P}_1 \leftarrow \emptyset, \mathcal{P}_2 \leftarrow \emptyset$ 
3  $\mathcal{P}_{gene} \leftarrow \text{NeuralSampler}(p_q, p_s)$ 
4 for  $p_i$  in  $\mathcal{P}_{gene}$  do
5    $e_{inter} \leftarrow \text{CalculateGrasp}(p_i, p_q, p_s, \mathcal{M})$ 
6    $\mathcal{E}_{inter}.\text{append}(e_{inter})$ 
7    $\mathcal{P}_1.\text{append}(p_i)$ 
8 end
9  $\mathcal{G}.\text{addNodes}(\mathcal{P}_1)$ 
10  $\mathcal{G}.\text{addEdges}(\mathcal{E}_{inter})$ 
11 for  $p_j$  in  $\mathcal{P}_{gene} \setminus \mathcal{P}_1$  do
12    $e_{intra} \leftarrow \text{CalculateGrasp}(p_j, \mathcal{P}_1, C_{\mathcal{P}_{gene} \setminus \mathcal{P}_1}^2, \mathcal{M})$ 
13   if  $\text{Connect}(p_q, p_j)$  then
14      $\mathcal{G}.\text{addNodes}(p_j)$ 
15      $\mathcal{G}.\text{addEdges}(e_{intra})$ 
16      $\mathcal{E}_{intra}.\text{append}(e_{intra})$ 
17      $\mathcal{P}_2.\text{append}(p_j)$ 
18   end
19 end
20 for  $p_k$  in  $\mathcal{P}_1$  do
21    $e_{intra} \leftarrow \text{CalculateGrasp}(C_{\mathcal{P}_1}^2, \mathcal{M})$ 
22    $\mathcal{G}.\text{addEdges}(e_{intra})$ 
23    $\mathcal{E}_{intra}.\text{append}(e_{intra})$ 
24 end
25 Return( $\mathcal{G}$ )
```

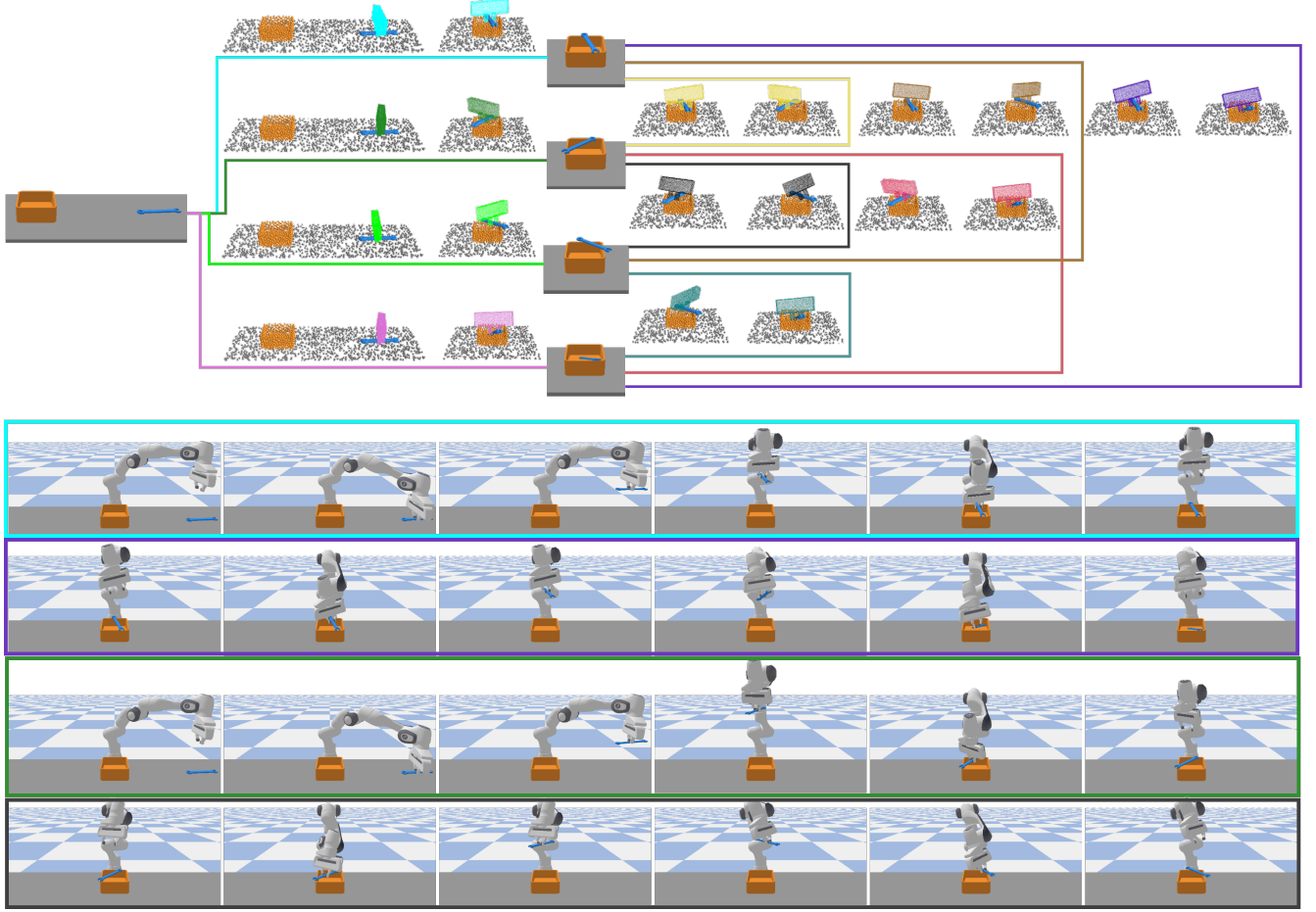


Fig. 3. An example of a manipulation graph. The intermediate stable placements are proposed by the generation models based on the segmented point clouds of the initial scene. The colored edges representing different shared grasp configurations connect the nodes in the graph. The relative position between the gripper and the wrench is invariable on each edge. Framed snapshots show the execution of reorienting the exemplary object, including the motion primitives of pick-up g_{xy}^{up} and place-down g_{xy}^{dn} .

In addition to predicting stable placements of objects, it is also important to realize the collision-free transformation between stable positions when the system uses supports to adjust the states of objects for manipulation tasks. It is challenging to adjust the object's pose from one stable placement state to another, especially in a highly constrained space. We solve this problem by computing shared grasp configurations connecting proposed stable placements and incorporating motion primitives of the robot to relax motion planning [1]. We propose a reorientation planner as described in Alg. 1 to build the manipulation graph \mathcal{G} , from which we can search for sequential pick-and-place operations to change the orientation of objects. Next, we discuss the implementation details.

The planner takes as input segmented point clouds of the query object p_q and the supporting environment p_s . In the beginning, the manipulation graph \mathcal{G} is initialized with the start scene $\mathcal{P} = (p_q \oplus p_s)$ (line 1). We take the model of the robot and the defaulted gripper \mathcal{M} as given. Here, we use a parallel-finger gripper, which can be replaced by a suction gripper. The *NeuralSampler* represents obtaining proposed placements introduced in Sec. III-A. In detail, $\mathcal{P}_{gene} = \{p_1, p_2, \dots, p_n\}$ is a set of generated point clouds, where one entry $p_i =$

$(p_q \mathbf{T}_q^i \oplus p_s)$ is a combination of the original supporting environment and the newly transformed object with proposed transformation $\mathbf{T}_q^i = [\mathbf{R}_q^i | \mathbf{t}_q^i]$.

The *CalculateGrasp* computes grasp configurations, which are comprised of shared contact points on two convertible placements, approaching directions of the gripper, and feasible kinematics of the robot in the world frame. The index of the query object's points is invariant to the transformation \mathbf{T}_q^i . Thus, the indexes of the transformed points $p_q \mathbf{T}_q^i$ are the same as the initial observation p_q . We can generate grasp points [26] on point clouds and determine shared contact points on the placements. We then examine the requirement of grasping force closure with the friction coefficient f at a pair of points (q_x, q_y) on the query object. The gripper's approaching directions \mathbf{d}_{xy} with respect to the world frame are sampled uniformly at the contact points (q_x, q_y) on a placement. Explicitly, the approaching directions \mathbf{d}_{xy}^i and \mathbf{d}_{xy}^j to two connected placements satisfy

$$\mathbf{d}_{xy}^i = \mathbf{d}_{xy}^j \cdot \mathbf{R}_i^j \quad (6)$$

where \mathbf{R}_i^j is the rotation matrix from the points $p_q \mathbf{T}_q^i$ to $p_q \mathbf{T}_q^j$ with respect to the world frame. Hence, the object pose is

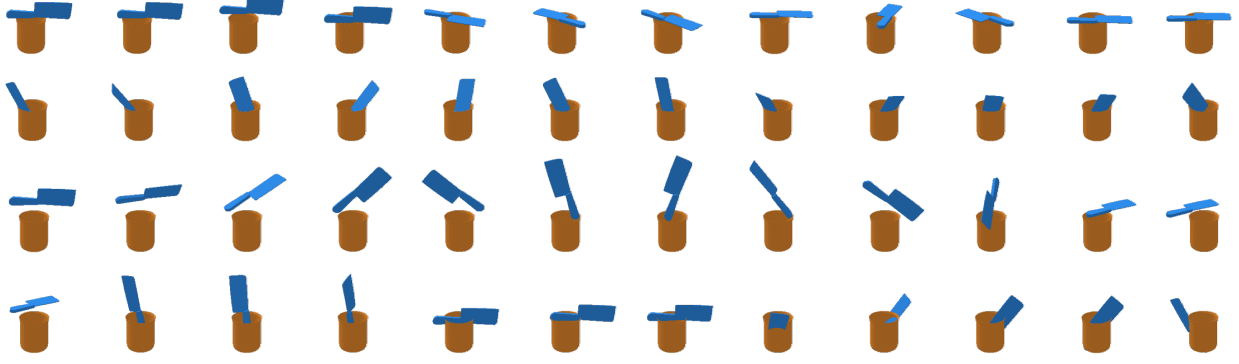


Fig. 4. Pose examples of an object-support pair. The top two rows show the stable placements afforded by the support after the variation tests. The object can be placed on the support or in the support. The bottom two rows display the unstable poses of the object. The object may separate from the support or contact the support in an unstable way or penetrate the support.

identical in the gripper frame. Two placements share the grasp configuration, which is the key to perform sequential pick-and-place operations. After that, we examine the reachability of the grasp $g_{xy} = ((q_x, q_y), \mathbf{d}_{xy})$ on two placements, respectively, by calculating the collision between the gripper \mathcal{M} and the supporting environment p_s as well as the object points. The calculation is performed in the gripper frame. We restrict the gripper's approaching directions to make the robot's kinematics above the flat table surface feasible. Namely, $\mathbf{d}_{xy} \cdot \mathbf{n} \leq 0$, where \mathbf{n} is the normal vector of the table surface. The robot kinematics is further examined given the pose g_{xy} of the gripper. The force-closure and feasible grasp configurations are added to the manipulation graph.

For expanding the manipulation graph, we first calculate shared grasp configurations between the initial state $(p_q \oplus p_s)$ and each transformed placement in \mathcal{P}_{gene} (lines 4-8). As per the *CalculateGrasp* calculation, if the grasp configurations linking the initial object pose and stable placements are found, we add the set of transformed placements \mathcal{P}_1 as new nodes and corresponding grasp configurations \mathcal{E}_{inter} as inter-edges to the manipulation graph \mathcal{G} (lines 9-10). Then, we examine the remaining placements in $\mathcal{P}_{gene} \setminus \mathcal{P}_1$ for connectivity with the initial state $(p_q \oplus p_s)$. In *CalculateGrasp*, we attempt to calculate grasp configurations which connect the remaining placements with the established nodes from the first step and link between the remaining placements. The results are intra-edges e_{intra} . When a placement p_j in $\mathcal{P}_{gene} \setminus \mathcal{P}_1$ is linked to the initial point cloud through intermediate placements, the p_j is added to the manipulation graph \mathcal{G} as a new node, and the associated shared grasp configurations e_{intra} are added to the grasp graph \mathcal{G} as intra-edges (lines 11-19). At last, we make the grasp graph complete with grasp configuration e_{intra} between the placements in \mathcal{P}_1 , which enables the graph to provide redundant manipulation paths for reorienting objects. Ultimately, the algorithm returns the grasp graph \mathcal{G} , from which we can determine a path to move the object from the initial pose to a pose that exposes the initially blocked functional part through intermediate placements afforded by an extrinsic support.

Fig. 3 gives an example of the manipulation graph. The

initial scene contains the wrench to be manipulated and the tray working as the support. The intermediate stable placements are proposed based on the point clouds of the initial scene. The shared grasp configurations connecting the nodes are also calculated in a sequence described in Alg. 1. We visualize the grasp configurations in terms of the segmented point clouds, where the gripper is located at the calculated poses. The relative position between the gripper and the wrench is invariable for every pick-and-place operation in the manipulation graph. As shown in Fig. 3, one shared grasp configuration associated with two stable nodes, which are linked with the same line, is identical in the gripper's frame. The gripper's poses are rendered in different colors for pick-and-place configurations in the manipulation graph. Also, the colors of different edges in the graph are associated with different grasp configurations.

In addition, similar to [1], we define motion primitives of the whole robot arm based on the shared grasp configurations for relaxing motion planning. The definitions of pick-up g_{xy}^{up} and place-down g_{xy}^{dn} are

$$g_{xy}^{up} = ((g_{xy}, \varepsilon, h) \rightarrow (g_{xy}, \varepsilon) \rightarrow g_{xy}), \quad (7)$$

$$g_{xy}^{dn} = ((g_{xy}, h) \rightarrow g_{xy} \rightarrow (g_{xy}, \varepsilon, h)), \quad (8)$$

where ε is the constrain of the two fingers, and h is the height above placements. The motion primitives are checked to make sure they are collision-free and IK-feasible. As depicted in Fig. 3, the motion primitives provide sufficient manipulation space for reorienting objects.

C. Data Generation

We generated a synthetic dataset containing point clouds of the object-support pairs' stable placements and unstable poses. The transformation pose sets from each state to all stable placements are calculated in the world frame. The mesh models used for the dataset generation are collected from 3D Warehouse¹. We examined each model's water tightness and convexity and resized the models to regular sizes. A total of

¹<https://3dwarehouse.sketchup.com/>

TABLE I
THE ABLATION TESTS OF VARIATIONS OF OUR MODELS

Models	Box+Axe		BeakerI+Spoon		Cup+Plier		HolderI+Plier		TrayI+Cutter		TrayII+Wrench		BeakerII+Razor		BeakerII+Knife		HolderII+Pen	
	rate(%)	types	rate(%)	types	rate(%)	types	rate(%)	types	rate(%)	types	rate(%)	types	rate(%)	types	rate(%)	types	rate(%)	types
StageI with s_1	66.7	18	33.3	6	50	7	11.5	3	43.5	10	38.1	8	33.3	6	26.7	4	26.7	4
StageI with s_2	100	11	/	0	100	4	/	0	100	1	100	1	100	1	100	3	100	2
Full model	88.1	59	85.7	12	90	9	100	10	89.3	25	100	5	82.4	14	87.5	14	87.5	7

We compare the full-model method with the single-stage methods. It is reasonable to choose placements with a higher threshold s_2 . Our full-model method with the refinement stage outperforms the single-stage method in obtaining more stable placements.

TABLE II
COMPARISON WITH THE MESH-BASED METHOD

Methods	Box+Axe		BeakerI+Spoon		Cup+Plier		HolderI+Plier		TrayI+Cutter		TrayII+Wrench		BeakerII+Razor		BeakerII+Knife		HolderII+Pen	
	time(s)	ratio	time(s)	ratio	time(s)	ratio	time(s)	ratio	time(s)	ratio	time(s)	ratio	time(s)	ratio	time(s)	ratio	time(s)	ratio
Ours	4.7	0.91	15.8	0.92	16.7	1.00	27.0	1.00	9.6	0.88	44.0	1.00	13.6	1.00	11.4	1.00	22.9	1.00
Mesh-based [5]	14.4	0.22	23.3	1.00	23.3	0.56	11.5	1.00	14.8	0.76	12.0	0.60	14.3	0.93	18.9	1.00	13.6	1.00

We compare our method based on point clouds with the mesh-based method on time cost and placement variation. The ratios of stable placements afforded by the support to the all predictions are listed. Our method is faster in predicting stable placements than the mesh-based method.

35 support and 136 objects are included, commonly used in daily and factory scenes.

The unstable poses and objects' stable placements afforded by supports are generated in Pybullet [27]. At first, the object falls freely above the support with random poses. We run these simulation processes for some time steps. After checking the contact relationship between two items and the dynamics of the object, we record stable placement poses. We observed penetration cases in the simulation, so these unstable poses are included in the dataset. Aiming to let the object's placement poses occupy both the feasible space and unfeasible space around the support as much as possible, we study the linear variation of the object's stable placements along with the axial directions of the world frame, as well as the orientation variation along with the axial directions of the object frame and the world frame. We obtain sufficient stable placements based on the same criterion for placement classification in the former step. Unstable poses are also recorded, including separation, penetration, and unstable contact cases. An example of an object-support pair's poses is depicted in Fig. 4. The poses are used to train discriminators, one to learn the boundary of penetration and stability and the other to learn the boundary of noncontact or unstable contact and stability. Considering the initial poses of the objects, we collected random positions of the objects placed next to the support on the working platform. Transformation poses $\{\mathbf{T}_{gt1}\} = (\{t_{gt1}\}, \{o_{gt1}\})$ from initial poses to stable placement poses and $\{\mathbf{T}_{gt2}\} = (\{t_{gt2}\}, \{o_{gt2}\})$ from unstable poses to stable placement poses are computed with respect to the world frame. In all, 314 pairs of object-support combinations containing ample stable placements are used.

IV. EXPERIMENTS

We perform simulation experiments and real-world experiments to evaluate our proposed methods. These experiments test (a) the accuracy of predicting stable placements for novel object-support pairs, (b) the diverse types of generated stable placements afforded by the supports, and (c) the connectivity of manipulation graphs.

Our networks are implemented in PyTorch and trained on an NVIDIA 1080Ti GPU. We use Adam as the optimizer. The training of generative models and discriminators finally converged.

A. Simulated Experiments

Simulation experiments are conducted in PyBullet. We first examine the performance of the trained models with a set of ablation experiments. Second, we compare our method with the mesh-based method [5] on time cost and placement diversity. As listed in Table I and Table II, novel combinations of objects and supports with various geometry are used for tests. The coupled items match in size and often appear together in respective scenes.

1) *Success rate of prediction*: To validate the performance of our two-stage method, we run ablation tests with variations of trained models on unseen object-and-support pairs. At the beginning of the simulation, the query object is placed on the table with a random pose next to the support, as shown in Fig. 2. We obtain segmented point clouds of the query object, the supporting item, and the table surface according to the color and depth images captured from multiple camera poses. Given point clouds of the initial scene, object poses are sampled using the learned distribution in the first stage. Then, we set the threshold δ_1 for the defined distance d to 0.003 and use the transformed point clouds with the weighted score s_1 higher than 0.5, where α is 0.5, and β is 0.5 for the two discriminators, respectively. Next, the selected poses are refined in the second stage, where the threshold δ_2 is set to 0.02. Finally, we obtain the predicted placements with the weighted score s_2 higher than 0.99.

We put the object at the predicted placement poses and then run the simulation for some time steps to allow the object to stabilize to the final poses. We compare the final poses with the predicted poses from our models. We also set thresholds for the object's position change in the simulation process. The thresholds for offset variation is 1cm, and orientation variation is 10°. If the final poses change within the thresholds compared with the predicted poses, we

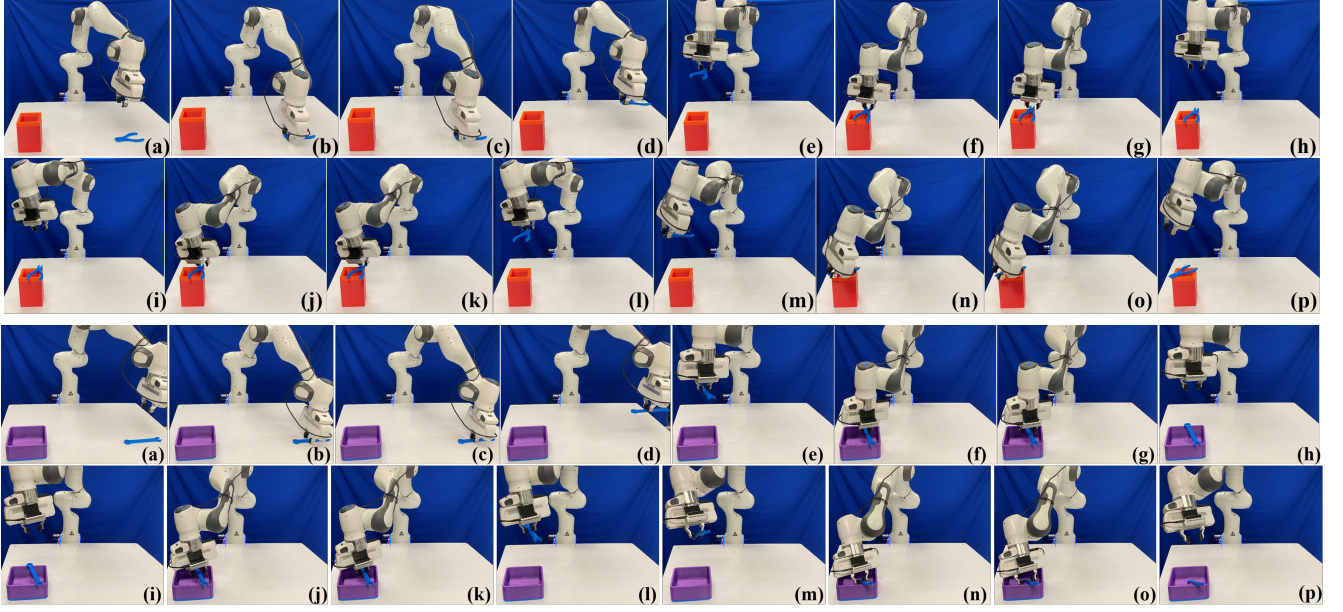


Fig. 5. Two real-world examples of reorienting objects with stable placements afforded by supports. In the top row of each example, the robot picks up the query object (the plier or the wrench) from the initial pose on the table and places the object on the support (the red holder or the purple tray) at one proposed placement pose. (a-h) is the first pick-and-place operation. Similarly, (i-p) is the second pick-and-place operation to adjust the object's pose to another placement afforded by the support. The robot performs collision-free sequential pick-and-place operations to reorient the objects with designed motion primitives.

believe that the predicted placement poses are stable. The results of the success rate obtained by different methods are reported in Table I. Results indicate that our method can generalize to novel object-support pairs with random start poses on the table. We can see that the first stage with a higher threshold of s_2 achieves a higher success rate than the first stage with s_1 . It is reasonable to choose predicted placements with s_2 higher than 0.99 according to the results of the stability rate. However, the strict constraint of the score limits the types of placements and even leads to 0 placement. Therefore, the refinement stage is necessary for generating sufficient placements for building the manipulation graph. Since the full-model method generate placements with larger variation ($\delta_2 > \delta_1$) than the single-stage methods, the full-model method does not outperform the others in terms of the accuracy rate in some cases. Nevertheless, the overall accuracy of our method exceeds 82.4%.

2) *Placement types*: Table I shows the numbers of nonredundant stable placement poses generated from the full-model method and its variations. Even if the distance threshold of the full-model method is a larger value δ_2 than the other two methods δ_1 , the full-model method generates more types of placements compared with single-stage methods in most cases. More stable placements are better for building the manipulation graph when the base of the robot arm is fixed in the environment, as more placements provide more grasp configurations for the robot to reorient the query objects. We also compare our placements types with the mesh-based method in [5]. The results are shown in Table II. In the mesh-based method, the object starts in random poses and is dropped above the support in simulation. As a result, this method requires detailed physical information of mesh models,

including the masses and the friction, to obtain stable placements. Our method takes the point clouds as input to predict stable placements in the construct. The ratios of placements afforded by the support are reported in Table II. The mesh-based method of obtaining placements by dropping is prone to generate placements afforded by both support and the table surface. In comparison, ours can obtain placements mostly supported by the support, which eliminates the instability caused by the table condition.

3) *Time cost*: Here, we compare the time cost of obtaining a placement with the work [5]. The mesh-based method takes 5s for each drop simulation experiment. After each trial, the stable placement contact with the support is recorded. We count the time cost by the two methods for obtaining the same number of placements for the same pair in Table I. The average time for obtaining one stable placement is reported in Table II. Our method equipped with the delicate card is faster in predicting stable placements than the mesh-based method. In general, ours costs less time to obtain enough stable poses.

B. Real Robot Experiments

We conduct real-world experiments using the Franka Emika Panda robot with the default parallel-jaw gripper, as shown in Fig. 1, to validate the connectivity of manipulation graphs. The Intel RealSense D435 camera is mounted on the end effector for point clouds perception. We employ the eye-in-hand calibration [28] to calibrate the transformation matrix between the end effector and the camera before capturing color images and depth images. We use ROS for the hardware communication of the robot and the camera. In the beginning, as depicted in Fig. 1, the query objects are placed on the table with random initial poses next to the supporting items.

Our system first constructs a scene by integrating a series of color images and depth images captured from different angles and simultaneously at each angle [29]. The pre-defined trajectory of the construction process is displayed in the accompanying video². The point clouds are then sampled from the constructed scene by Farthest Point Sampling [23]. Segmentation masks for different instances are determined by using [21]. After obtaining segmented point clouds, the world frame with directions of axes corresponding to the canonical pose is set at the center of the support's bottom. We use the trained models to generate objects' placements and then calculate motion primitives in the manipulation graphs with respect to the world frame.

Fig. 5 shows real-world execution of reorienting objects with a branch of sequential pick-and-place operations in the manipulation graphs. According to the graphs, the robot first adjusts the grasp direction above the object (a). Then the robot reaches the object and closes the two-finger gripper to grasp the object (b, c). Next, the robot picks up the object to leave enough space for adjusting the object's state and moves the object to the position above a new placement (d, e). Then the robot places the object down to the new placement and opens the gripper (f, g). Finally, the robot moves away from the object. Repeatedly, the robot performs pick-and-place operations (h-p) to move the object to new placements. The motion planning between motion primitives is based on RRT-Connect [30]. Videos of real robot experiments are in the following link³. The robot can reorient objects without collision. We showcase that our method is capable of reorienting the query object to multiple placements in case of different manipulation tasks. As the robot is fixed in the environment, multiple stable placements can help to find feasible paths to reorient the query object. Since the grasp points prediction is not accurate enough for grasping objects with different geometry, we also found cases of changing the object pose relative to the gripper when the robot grasps the object, which can be improved by utilizing accurate grasp methods.

V. CONCLUSION

We propose a data-driven method to predict objects' stable placements afforded by supporting items. Moreover, we build manipulation graphs based on the point clouds, containing collision-free pick-and-place operations for reorienting objects. A large-scale dataset covering as many contact cases between objects as possible is generated for training. The experiments prove the effectiveness of our method in both simulated and real environments. In future work, we will utilize deep learning methods to couple objects and supports with suitable sizes and placement poses in a cluster environment. We will also use mobile manipulation methods to grasp the object with more feasible paths than using a robot with a fixed base in the environment.

²<https://drive.google.com/file/d/1cCeE67lvJyidZLKYzQcV111yNvol4PQf/view?usp=sharing>

³<https://drive.google.com/file/d/1PXi5kzlpMVhWY9OGrQmQfrD6b2WKgA/view?usp=sharing>

ACKNOWLEDGEMENT

The work is supported by the Shenzhen Key Laboratory of Robotics Perception and Intelligence, Southern University of Science and Technology, Shenzhen 518055, China, under Grant ZDSYS20200810171800001.

REFERENCES

- [1] W. Wan, H. Igawa, K. Harada, H. Onda, K. Nagata, and N. Yamanobe, "A regrasp planning component for object reorientation," *Autonomous Robots*, vol. 43, no. 5, pp. 1101–1115, 2019.
- [2] S. Yuan, L. Shao, C. L. Yako, A. Gruebele, and J. K. Salisbury, "Design and control of roller grasper v2 for in-hand manipulation," in *2020 IEEE/RSJ International Conference on Intelligent Robots and Systems (IROS)*, pp. 9151–9158, IEEE, 2020.
- [3] T. Li, K. Srinivasan, M. Q.-H. Meng, W. Yuan, and J. Bohg, "Learning hierarchical control for robust in-hand manipulation," in *2020 IEEE International Conference on Robotics and Automation (ICRA)*, pp. 8855–8862, IEEE, 2020.
- [4] C. Cao, W. Wan, J. Pan, and K. Harada, "Analyzing the utility of a support pin in sequential robotic manipulation," in *2016 IEEE International Conference on Robotics and Automation (ICRA)*, pp. 5499–5504, IEEE, 2016.
- [5] J. Ma, W. Wan, K. Harada, Q. Zhu, and H. Liu, "Regrasp planning using stable object poses supported by complex structures," *IEEE Transactions on Cognitive and Developmental Systems*, vol. 11, no. 2, pp. 257–269, 2018.
- [6] J. A. Haustein, K. Hang, J. Stork, and D. Kragic, "Object placement planning and optimization for robot manipulators," in *2019 IEEE/RSJ International Conference on Intelligent Robots and Systems (IROS)*, pp. 7417–7424, IEEE, 2019.
- [7] J. A. Haustein, S. Cruciani, R. Asif, K. Hang, and D. Kragic, "Placing objects with prior in-hand manipulation using dexterous manipulation graphs," in *2019 IEEE-RAS 19th International Conference on Humanoid Robots (Humanoids)*, pp. 453–460, IEEE, 2019.
- [8] Y. Hou, Z. Jia, and M. T. Mason, "Reorienting objects in 3d space using pivoting," *arXiv preprint arXiv:1912.02752*, 2019.
- [9] Y. You, L. Shao, T. Migimatsu, and J. Bohg, "Omnihang: Learning to hang arbitrary objects using contact point correspondences and neural collision estimation," *arXiv preprint arXiv:2103.14283*, 2021.
- [10] C. Paxton, C. Xie, T. Hermans, and D. Fox, "Predicting stable configurations for semantic placement of novel objects," *arXiv preprint arXiv:2108.12062*, 2021.
- [11] B. Sundaralingam and T. Hermans, "Geometric in-hand regrasp planning: Alternating optimization of finger gaits and in-grasp manipulation," in *2018 IEEE International Conference on Robotics and Automation (ICRA)*, pp. 231–238, IEEE, 2018.
- [12] W. Wan, K. Harada, and F. Kanehiro, "Preparatory manipulation planning using automatically determined single and dual arm," *IEEE Transactions on Industrial Informatics*, vol. 16, no. 1, pp. 442–453, 2019.
- [13] S. Cruciani, K. Hang, C. Smith, and D. Kragic, "Dual-arm in-hand manipulation and regrasp using dexterous manipulation graphs," *arXiv preprint arXiv:1904.11382*, 2019.
- [14] W. Wan and K. Harada, "Achieving high success rate in dual-arm handover using large number of candidate grasps, handover heuristics, and hierarchical search," *Advanced Robotics*, vol. 30, no. 17–18, pp. 1111–1125, 2016.
- [15] W. Wan and K. Harada, "Reorientating objects with a gripping hand and a table surface," in *2015 IEEE-RAS 15th International Conference on Humanoid Robots (Humanoids)*, pp. 101–106, IEEE, 2015.
- [16] Z. J. Yifan Hou and M. T. Mason, "Fast planning for 3d any-pose-reorienting using pivoting," in *Proceedings of (ICRA) International Conference on Robotics and Automation*, pp. 1631 – 1638, IEEE Robotics and Automation Society (RAS), May 2018.
- [17] Y. Jiang, M. Lim, C. Zheng, and A. Saxena, "Learning to place new objects in a scene," *The International Journal of Robotics Research*, vol. 31, no. 9, pp. 1021–1043, 2012.
- [18] Y. Jiang, C. Zheng, M. Lim, and A. Saxena, "Learning to place new objects," in *2012 IEEE International Conference on Robotics and Automation*, pp. 3088–3095, IEEE, 2012.
- [19] L. Berscheid, P. Meißner, and T. Kröger, "Self-supervised learning for precise pick-and-place without object model," *IEEE Robotics and Automation Letters*, vol. 5, no. 3, pp. 4828–4835, 2020.

- [20] S. Cheng, K. Mo, and L. Shao, "Learning to regrasp by learning to place," *arXiv preprint arXiv:2109.08817*, 2021.
- [21] R. B. Rusu and S. Cousins, "3D is here: Point Cloud Library (PCL)," in *IEEE International Conference on Robotics and Automation (ICRA)*, (Shanghai, China), May 9-13 2011.
- [22] I. Goodfellow, J. Pouget-Abadie, M. Mirza, B. Xu, D. Warde-Farley, S. Ozair, A. Courville, and Y. Bengio, "Generative adversarial nets," *Advances in neural information processing systems*, vol. 27, 2014.
- [23] C. R. Qi, L. Yi, H. Su, and L. J. Guibas, "Pointnet++: Deep hierarchical feature learning on point sets in a metric space," *arXiv preprint arXiv:1706.02413*, 2017.
- [24] H. Fan, H. Su, and L. J. Guibas, "A point set generation network for 3d object reconstruction from a single image," in *Proceedings of the IEEE conference on computer vision and pattern recognition*, pp. 605–613, 2017.
- [25] Y. Rubner, C. Tomasi, and L. J. Guibas, "The earth mover's distance as a metric for image retrieval," *International journal of computer vision*, vol. 40, no. 2, pp. 99–121, 2000.
- [26] L. Shao, F. Ferreira, M. Jorda, V. Nambiar, J. Luo, E. Solowjow, J. A. Ojea, O. Khatib, and J. Bohg, "Unigrasp: Learning a unified model to grasp with multifingered robotic hands," *IEEE Robotics and Automation Letters*, vol. 5, no. 2, pp. 2286–2293, 2020.
- [27] E. Coumans and Y. Bai, "Pybullet, a python module for physics simulation for games, robotics and machine learning," 2016–2020.
- [28] R. Y. Tsai, R. K. Lenz, *et al.*, "A new technique for fully autonomous and efficient 3 d robotics hand/eye calibration," *IEEE Transactions on robotics and automation*, vol. 5, no. 3, pp. 345–358, 1989.
- [29] Q.-Y. Zhou, J. Park, and V. Koltun, "Open3D: A modern library for 3D data processing," *arXiv:1801.09847*, 2018.
- [30] J. J. Kuffner and S. M. LaValle, "Rrt-connect: An efficient approach to single-query path planning," in *Proceedings 2000 ICRA. Millennium Conference. IEEE International Conference on Robotics and Automation. Symposia Proceedings (Cat. No. 00CH37065)*, vol. 2, pp. 995–1001, IEEE, 2000.